



Nanofibres of CA/PAN with high amount of carbon nanotubes by core-shell electrospinning

Milana Lisunova*, Attila Hildmann, Benjamin Hatting, Vitaliy Datsyuk, Stephanie Reich

Freie Universität Berlin, Fachbereich Physik, Arnimallee 14, 14195 Berlin, Germany

ARTICLE INFO

Article history:

Received 25 March 2010

Received in revised form 25 June 2010

Accepted 4 July 2010

Available online 27 July 2010

Keywords:

A. Carbon nanotubes
A. Polymers
A. Fibres
E. Electro-spinning
B. Thermal properties

ABSTRACT

We prepared polyacrylonitrile (PAN) and cellulose acetate (CA) based nanofibres with high amount of carbon nanotubes (CNTs) by core-shell electrospinning. Atomic force microscopy (AFM) and transmission electron microscopy (TEM) were used to evaluate the morphology and structure of the electrospun nanofibres. Raman spectroscopy (Raman) and TEM indicate alignment of CNTs in the polymer fibres. Core-shell electrospinning improved the distribution and uniformity of the fibres. The loading of carbon nanotubes showed better thermal stability.

© 2010 Elsevier Ltd. All rights reserved.

1. Introduction

Electrospinning of cellulose and derived materials is a well known and well developed process for the production of nanofibres. Such fibres are used as filters, drug-delivery vehicles, and scaffolds for tissue cultures [1,2]. Electrospun cellulose acetate (CA) nanofibres with conductive fillers such as carbon nanotubes (CNTs) [3] are also interesting for electro-active paper sensor and actuator [1]. CA/CNTs – based composites are promising materials for sensors, electromagnetic shielding materials, and antistatic films [4], due to the unique electronic, thermal, optical, and mechanical properties of CNTs [3]. Additionally, carbon nanotubes were considered for a wide range of applications in nanotechnology, because of their superior material properties such as low density and high aspect ratio [5]. Electrospinning CA solution with a filler fraction greater than 4 wt.% resulted in the formation of short and beaded fibres [4]. Electrospinning CA with high concentration of CNTs was limited by viscosity [6]. Incorporating a high fraction of filler in electrospun CA nanofibres was achieved by adding polyacrylonitrile (PAN) or polyethylene oxide (PEO) [7]. Such blending of polymers leads to the enhancement of the homogeneity and the stability of the electrospun jet, but the immiscibility of polymers is problematic [7]. Core-shell electrospinning seems to be promising for combining immiscible polymer solutions while keeping their individual properties [8–12].

In this work we report the production of core-shell nanofibres based on cellulose acetate and polyacrylonitrile filled with a large fraction of carbon nanotubes. We investigate and discuss the morphology, structure and thermal stability of the nanofibres.

2. Experimental

2.1. Materials

The CNTs used in this work were multiwalled carbon nanotubes (MWCNTs) “Baytubes C150P” supplied by Bayer Materials Science AG. The MWCNTs were synthesized by the chemical vapour deposition (CVD). Statistical study of the TEM images (Fig. 1) of CNT showed they are multiwalled nanotubes with an outer diameter d 20–40 nm and their length l_n is about tens of microns (μm). The density of the MWCNT walls was estimated according to the ENI 8060 $\rho_f = 1.2\text{--}1.7 \text{ g/cm}^3$.

Cellulose acetate (CA, with density $\rho_{in} = 1.184 \text{ g/cm}^3$, melting temperature $T_m = 280 \text{ }^\circ\text{C}$) and polyacrylonitrile (PAN, with density $\rho_{in} = 1.184 \text{ g/cm}^3$, melting temperature $T_m = 317 \text{ }^\circ\text{C}$) were obtained from Aldrich. The *N,N*-dimethyl-formamide (DMF), dimethyl-acetamide (DMAc) and acetone (Ac) were purchased from Aldrich and used without any purification as solvents with boiling points $T_b = 153 \text{ }^\circ\text{C}$, $T_b = 164 \text{ }^\circ\text{C}$ and $T_b = 56 \text{ }^\circ\text{C}$, respectively.

2.2. Electrospinning setup

A schematic illustration of the experimental setup for electrospinning is presented in Fig. 2. Coaxial needles containing the core

* Corresponding author. Tel.: +49 30 838 52155; fax: +49 30 838 56081.
E-mail address: milana.lisunova@fu-berlin.de (M. Lisunova).

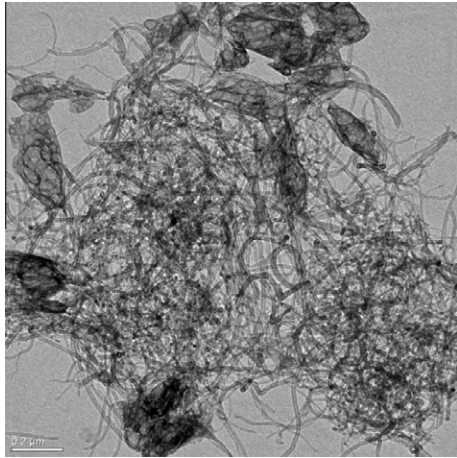


Fig. 1. Typical TEM image of multiwalled carbon nanotubes.

and shell precursor solutions were used to produce the fibres. 10 wt.% of PAN in DMF with 15 wt.% of CNTs was used to produce the PAN/CNTs fibres. Fifteen weight percent of CA in DMAc/acetone (2–1) and 10 wt.% of PAN in DMF with 35 wt.% of CNTs were used to produce the core and shell of the CA/PAN–CNTs nanofibres, respectively. The fraction of nanotubes in both samples is given to the polymer matrix. The flow rates of both solutions were 0.2 ml/h. The tip of the core needle and the collector were connected to the high-voltage power supply. The tip-to-collector distance was 15–20 cm, and the electrical potential difference was 30 kV.

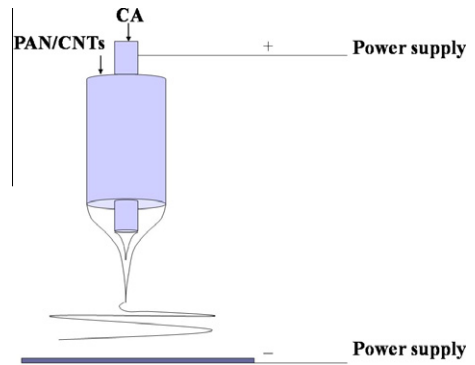


Fig. 2. Schematic illustration of the electrospinning setup.

2.3. Characterization

The calorimetry experiments were performed using a differential-scanning calorimeter DSC-PT1 (Linseis Messgeräte GmbH), equipped with sub-ambient temperature operation. The heat flux and temperature were calibrated with a sapphire standard for the same scan rate as used in our experiments. The measurements were carried out in the temperature range of 350–678 K, in the heating mode. The samples were encapsulated into small-volume aluminum hermetic pans. In order to keep the melt peaks as narrow as possible, the masses of samples were only 2–3 mg.

The structure of MWCNTs and the MWCNTs/PAN nanofibres were examined using the TEM (JEM 100 °C, Jeol, operating at accelerating voltage 100 kV). The surface morphology of the nanofibres

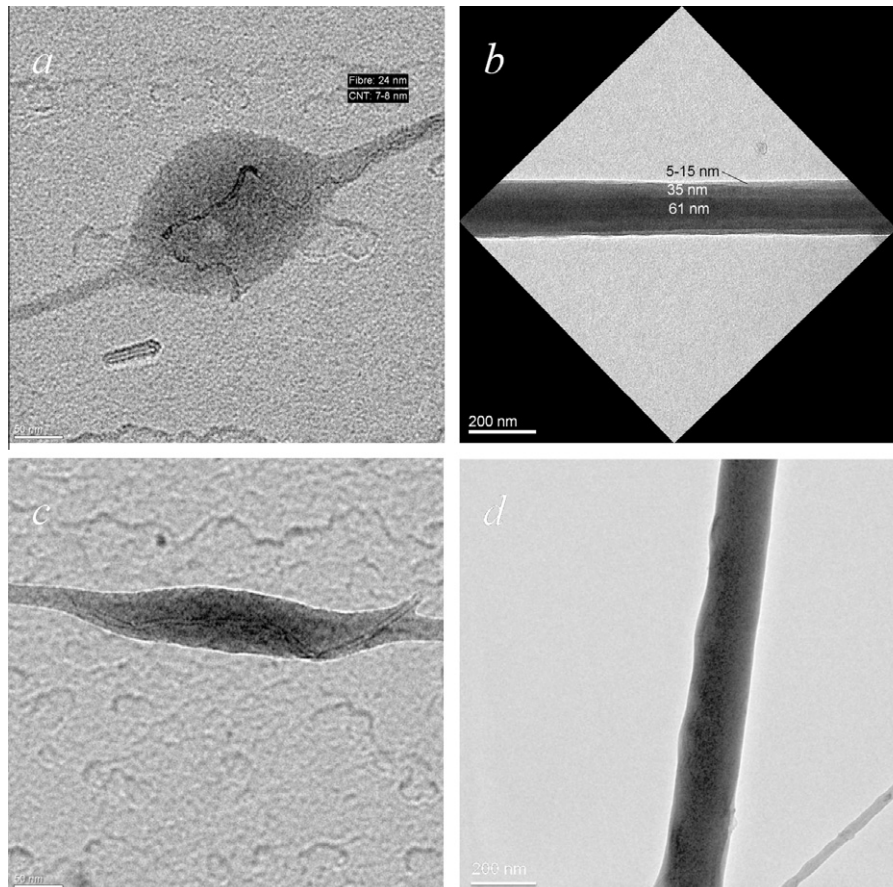


Fig. 3. TEM images of the PAN/CNTs (a and c) and CA/PAN–CNTs (b and d) nanofibres.

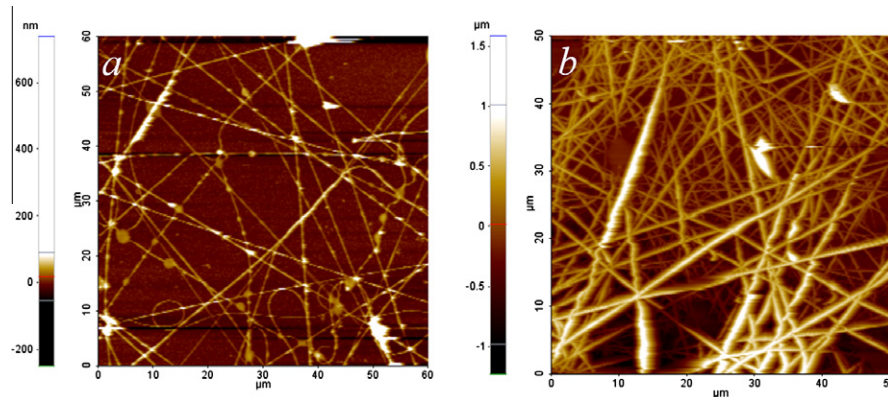


Fig. 4. AFM images of the PAN/CNTs (a) and CA/PAN-CNTs (b) nanofibers.

was studied by atomic force microscopy (AFM, Park AFM, Schaefer Technologie GmbH). Raman spectroscopic analysis of MWCNTs/PAN nanofibres was carried out using the Xplora Raman spectrometer (Horiba Scientific), under ambient conditions. The 514.5 nm line from an Ar⁺ laser was used for excitation at a power of 6 mW. Ultrasonication was conducted using a sonifier equipped with a cup horn Sonopuls HD3100 (Bandelin), which was operated at a frequency of 10 kHz with output power 100 W. The CNTs in polymer solution were sonicated for 30 min.

3. Results and discussion

3.1. Morphology

Fig. 3 presents the already introduced TEM images of the PAN/CNTs (a and c) and CA/PAN-CNTs (b and d) composites. The fraction of nanotubes is the same in both samples (15 wt.%); the fibres were prepared by electrospinning (Fig. 3a and c) and core-shell electrospinning (Fig. 3b and d). Examination of the images reveals that the MWCNTs are homogeneously distributed inside the polymeric fibres and aligned along the axes of the nanofibres. The alignment of CNTs by electrospinning was also investigated by Gogotsi et al. [13–15]. According to their hypothesis alignment of CNTs in the nanofibre occurs through two mechanisms: flow-confinement and charge-induced alignment during the electrospinning process.

Investigation of the surface morphology by AFM (see Fig. 4) shows that core-shell electrospinning leads to the formation of more smooth fibres compared to the fibres produced by electrospinning in Fig. 4a. Moreover, it is clearly proved that the core-shell structure reduced the amount of beads and defects. The effect of core-shell electrospinning on the distribution and packing of the fibre was also reported by Han et al. [9]. Well defined and uniform fibres were observed for the combination of Nylon-6 (core)-polyurethane (shell) [9], poly(ethylene oxide) (shell) and polysulfone (core) [10], poly(methyl methacrylate) (core) and poly(3-hexylthiophene) (shell) [11], poly(2-methoxy-5-(2-ethylhexyloxy)-1,4-phenylenevinylene) (core) and poly(vinyl pyrrolidone) (shell) [12].

The estimated diameters were about 40–50 nm PAN/CNTs and 150 nm for the CA/PAN-CNTs nanofibres. The thicker diameter of the CA/PAN-CNTs results from the structural organization with an inner diameter of CA (core) around 60 nm and outer layer of PAN-CNTs (shell) around 50 nm.

The Raman spectra of the CA/PAN-CNTs nanofibres in Fig. 5 confirmed the embedding of CNTs. The strongest peak at 1580 cm⁻¹ (G peak), corresponds to scattering on sp² bounded carbon atoms combined into graphite clusters. The D peak centered at 1350 cm⁻¹ is characteristic of the scattering on disordered graph-

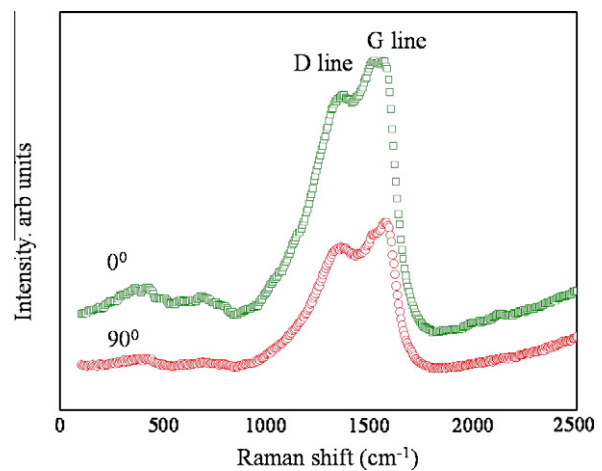


Fig. 5. Raman spectra of CA/PAN-CNTs nanofibres for the polarization parallel (□) and perpendicular (○) to the fibre axis.

ite-like carbon clusters (sp³ bonded carbon atoms). The intensity of the G and D bands is highest when the polarization is parallel to the fibre axis while it is lowest when it is perpendicular. Such reduction of the intensity of Raman signals indicates that the carbon nanotubes are aligned preferentially along the fibre axis [16–19].

3.2. DSC of electrospun nanofibres

Fig. 6 compares the DSC curves for fibres made for PAN (1), CA (2) and PAN/MWCNTs (3) and CA/PAN-CNTs (4) composites (scan rate 10 K/min). The exothermic peaks of the PAN, PAN/MWCNTs and PAN/CA/MWCNTs electrospun nanofibres (310–320 °C) are attributed to the melting point of PAN. The melting temperature of PAN slightly increases (10 K) with MWCNTs incorporation which is probably due to the good dispersion of MWCNTs and the large contact area of the MWNTs and PAN molecules.

The exothermic peak within the range 350–360 °C observed in CA and CA/PAN-CNTs corresponds to the crystallization temperature T_c of CA or the molecular rearrangement in the fibre. The degradation temperature of CA/PAN-CNTs is higher than pure CA. This is mainly due to the structural organization of the fibres. The CA/PAN-CNTs consists of CA core covered by thin layer of PAN with CNTs, which increases physical barrier for thermal transmission of the confined molecules during the thermal degradation of the fibres (see schematic representation in Fig. 6b) [5,20].

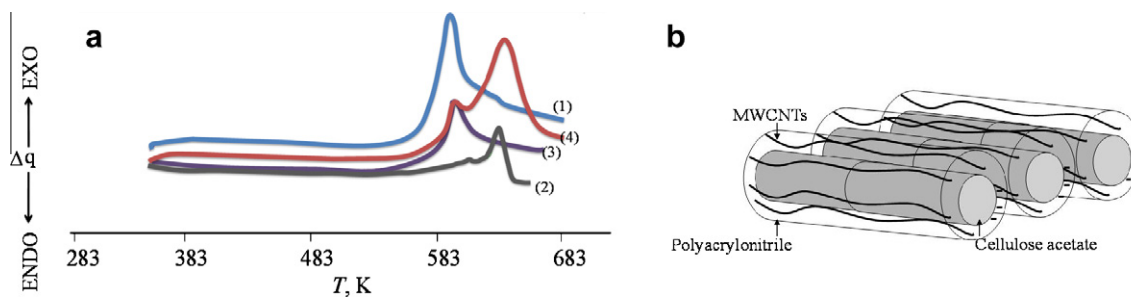


Fig. 6. DSC curves of PAN (1), CA (2), PAN/CNTs (3) and CA/PAN-CNTs (4) at 10 K/min heating rate (a). Schematic representation of CA/PAN-CNTs nanostructure (b).

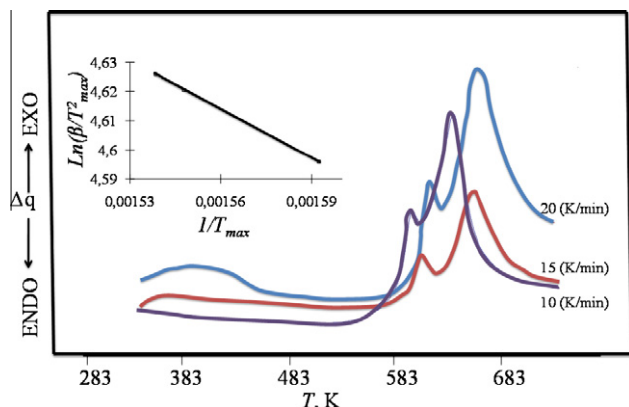


Fig. 7. DSC curves of CA/PAN-CNTs nanofibers at 10, 15, 20 K/min heating rates. The insert shows Kissinger plot for the second peaks of CA/PAN-CNTs nanofibers.

Table 1

The activation energies for electrospun PAN, CA, PAN/CNTs and CA/PAN-CNTs.

	E_a (kJ/mol)	
PAN	$E_{a, PAN} \approx 4299$	
PAN/CNTs	$E_{a, PAN} \approx 4361$	
CA	$E_{a, PAN} \approx 4598$	
CA/PAN-CNTs	$E_{a, PAN} \approx 4316$	$E_{a, CA} \approx 4602$

DSC curves of CA/PAN-CNTs obtained with a heating rate of 10, 15 and 20 K/min are presented in Fig. 7. The dependence between the temperature at which the reaction rate attain a maximum value and the heating rate is described by the Kissinger relationship

$$E_a = -R(\delta \ln \beta / T^2) / (\delta 1/T')$$

where T' is the temperature at peak maximum in the DSC response curve, β represents the heating rate of the sample and R is the universal gas constant.

The activation energy of degradation ΔE_a of PAN increases with CNTs loading (see Table 1). This result can be explained by the energy barrier numbers in the transport process; it is in agreement with previously reported data for sodium aluminum hydride and lithium aluminum hydride composites filled by CNTs. ΔE_a of CA slightly increases, i.e., CNTs are not included into the morphological structure of CA. The improved ΔE_a of PAN also confirms the deagglomeration and uniform distribution of CNTs [20–23].

4. Conclusion

Core-shell electrospinning improves the homogeneous distribution and uniformity of fibres based on PAN and CA with a high amount of CNTs. DSC data reveal an increase of the degradation

temperature for CA and PAN with CNTs loading. The improved thermal properties possibly reflect the deagglomeration and alignment of CNTs in the polymer fibres. The enhancement of activation energies of degradation of polymer fibres are believed to be due to the ordered structure of CNTs.

Acknowledgements

This work was supported by the BMBF Project Format CNTherm. The authors thank Solve Soren for the TEM investigation.

References

- [1] Liu H, Hsieh Y-L. Ultrafine fibrous cellulose membranes from electrospinning of cellulose acetate. *J Polym Sci B: Polym Phys* 2002;40:2119–29.
- [2] Pankonien AM. Electrospinning of cellulose and carbon nanotube-cellulose fibers for smart applications. Undergraduate thesis, University of Texas, Department of Aerospace engineering; 2008.
- [3] Reich S, Thomsen C, Maultzsch J. Carbon nanotubes: basic concepts and physical properties. Berlin: Wiley-VCH; 2004.
- [4] Rubenstein D, Han D, Goldgraben S, El-Gendi H, Gouma P, Frame MD. Bioassay chamber for angiogenesis with perfused explanted arteries and electrospun scaffolding. *Microcirculation* 2007;14(7):723–37.
- [5] Lisunova MO, Mamunya YP, Lebovka NI, Melezhyk AV. Percolation behaviour of ultrahigh molecular weight polyethylene/multi-walled carbon nanotubes composites. *Eur Polym J* 2007;43:949–58.
- [6] Seoul C, Kim Y-T. Electrospinning of Poly(vinylidene fluoride)/dimethylformamide solutions with carbon nanotubes. *J Polym Sci B: Polym Phys* 2003;41:1572.
- [7] Chen L, Bromberg L, Hatton TA, Rutledge GC. Electrospun cellulose acetate fibers containing chlorhexidine as a bactericide. *Polymer* 2008;48:1266–75.
- [8] Lallave M, Bedia J, Ruiz-Rosas R, Rodriguez-Mirasol J, Cordero T, Otero JC, et al. Filled and hollow carbon nanofibers by coaxial electrospinning of alcell lignin without binder polymers. *Adv Mater* 2007;19:4292–6.
- [9] Han X, Huang Z, He C, Liu L. Preparation and characterization of core-shell structured nanofibers by coaxial electrospinning. *High Perform Polym* 2007;19:147–59.
- [10] Sun Z, Zussman E, Yarin AL, Wendorff JH, Greiner A. Compound core-shell polymer nanofibers by co-electrospinning. *Adv Mater* 2003;15(22):1929–32.
- [11] Kuo C, Wang CT, Chen WC. Poly(3-hexylthiophene)/poly(methyl methacrylate) core-shell electrospun fibers for sensory applications. *Macromol Symp* 2009;279:41–7.
- [12] Li D, Babel A, Jenekhe SA, Xia Y. Nanofibers of conjugated polymers prepared by electrospinning with a two-capillary spinneret. *Adv Mater* 2004;16(22):2062–6.
- [13] Ko F, Gogotsi Y, Ali A, Naguib N, Ye H, Yang G, et al. Electrospinning of continuous carbon nanotube-filled nanofiber yarns. *Adv Mater* 2003;15(14):1161–5.
- [14] Lakoubovskii K. Techniques of aligning carbon nanotubes. *Cent Eur J Phys* 2009;7(4):645–53.
- [15] Zhou W, Wu Y, Wie F, Luo G, Qian W. Elastic deformation of multiwalled carbon nanotubes in electrospun MWCNTs-PEO and MWCNTs-PVA nanofibers. *Polymer* 2005;46:12689–95.
- [16] Anglaret E, Righi A, Sauvajol JL, Bernier, Vigolo B, Poulin P. Raman study of orientational order in fibers of single wall carbon nanotubes. *Physica B* 2002;323:38–43.
- [17] Liu T, Kumar S. Quantitative characterization of SWNT orientation by polarized Raman spectroscopy. *Chem Phys Lett* 2003;378:257–62.
- [18] Salalha W, Dror Y, Khalfin RL, Cohen Y, Yarin AL, Zussman E. Single-walled carbon nanotubes embedded in oriented polymeric nanofibers by electrospinning. *Langmuir* 2004;20:9852–5.
- [19] Rao AM, Saito R. Polarized Raman study of aligned multiwalled carbon nanotubes. *Phys Rev Lett* 2000;84(8):1820–3.

- [20] Lebovka N, Dadakova T, Lysetskiy L, Melezhyk O, Puchkovska G, Gavrilko T, et al. Phase transitions, intermolecular interactions and electrical conductivity behavior in carbon multiwalled nanotubes/nematic liquid crystal composites. *J Mol Struct* 2008;887:135–43.
- [21] Gong XY, Liu J, Baskaran S, Voise RD, Young JS. Surfactant-assisted processing of carbon nanotube/polymer composites. *Chem Mater* 2000;12:1049–52.
- [22] Cadek M, Coleman JN, Barron V, Hedicke K, Blau WJ. Morphological and mechanical properties of carbon-nanotube-reinforced semicrystalline and amorphous polymer composites. *Appl Phys Lett* 2002;81:5123.
- [23] Kim HS, park BH, Yoon JS, Jin H-J. Thermal and electrical properties of poly(l-lactide)-graft-multiwalled carbon nanotube composites. *Eur Polym J* 2007;5:1729–35.